HHS Public Access

Author manuscript

ASAIO J. Author manuscript; available in PMC 2024 September 01.

Published in final edited form as:

ASAIO J. 2023 June 01; 69(6): 569–575. doi:10.1097/MAT.0000000000001886.

von Willebrand Factor and Angiopoietin-2 are Sensitive Biomarkers of Pulsatility in CF-VAD Patients

Khanh T. Nguyen[1,2], **Jana Hecking**[2], **Ian C. Berg**[2], **Ramaswamy Kannappan**[2], **Esraa Ismail**[3], **Xuanhong Cheng**[3], **Guruprasad A. Giridharan**[4], **Palaniappan Sethu**[1,2]

[1]Department of Biomedical Engineering, School of Engineering and School of Medicine, The University of Alabama at Birmingham, Birmingham, AL

[2]Division of Cardiovascular Disease, School of Medicine, The University of Alabama at Birmingham, Birmingham, AL

[3]Department of Bioengineering and Material Science, School of Engineering, Lehigh University, Bethlehem, PA

[4]Department of Bioengineering, School of Engineering, University of Louisville, Louisville, KY

Abstract

Non-surgical bleeding occurs in a significant proportion of patients implanted with Continuous-Flow Ventricular Assist Devices (CF-VAD), which has been associated with diminished pulsatility. An in-vitro vessel-on-a-chip model, the Vascular Pulse Pressure Model (VPPM), with adult human aortic endothelial cells (HAECs) was used to identify biomarkers that are sensitive to changes in pulsatility. Diminished pulsatility resulted in an ~ 45% decrease in von Willebrand Factor (vWF) levels from 9.80 ng/mL to 5.32 ng/mL ($n=5$, $p<0.05$) and a 3-fold increase in Angiopoeiten-2 (ANGPT-2) levels from 775.29 pg/mL to 2471.93 pg/mL ($n=5$, $p<0.05$) in cultured HAECs. These changes are in agreement with evaluation of patient blood samples obtained pre-CF-VAD implant and 30-days post implant: a decrease in plasma vWF level by 50% from ~ 45.59 μg/mL to ~ 22.49 μg/mL ($n=15$, $p<0.01$) and a 64% increase in plasma ANGPT-2 level from 7,073 pg/mL to 11,615 pg/mL ($n=8$, $p<0.05$). Given shortcomings associated with animal models, in-vitro models that use human cells have great potential to determine the effects of changes in pulsatility. This study identified vWF and ANGPT-2 as highly sensitive to changes in pulsatility, in addition to Interleukin-6 (IL-6), IL-8 and Tumor Necrosis-α (TNF-α). These biomarkers may help identify patients who are at high risk of non-surgical bleeding events and determine optimal level of pulsatility.

Corresponding Author: Palaniappan Sethu, Department of Biomedical Engineering and Division of Cardiovascular Diseases, School of Engineering and School of Medicine, The University of Alabama at Birmingham, 1918 University Blvd, MCLM 290A, Birmingham, AL 35223 (USA), psethu@uabmc.edu.

Author Contributions

P.S., G.A.G, X.C and K.T.N developed the study conception and design. K.T.N, J.H and I.C. contributed to the fabrication of microfluidic devices, VPPM setup, data collection and data analysis. K.T.N, J.H, and R.K contributed to the collection and processes of patient blood samples and culture of patient-derived cells. K.T.N prepared draft manuscripts with written input from J.H, E.I., R.K, X.C., G.A.G, and P.S. All authors reviewed the study results and approved the final version of the manuscript.

Conflict of Interests: G.A.G. has served as a consultant and unpaid scientific advisor for NuPulseCV, but this manuscript does not directly pertain to the device of NuPulseCV. All other authors have no conflict of interest.

Keywords

Diminished pulsatility; Continuous Flow Ventricular Assist Device; non-surgical bleeding; Human Aortic Endothelial Cells; Angiopoietin-2; von Willebrand Factor

INTRODUCTION

Left Ventricular Assist Devices (LVADs) have become a valuable therapeutic option for patients with advanced heart failure (HF), both as a bridge-to-transplantation and as destination therapy, due to the paucity of donor organs (McLarty, 2015; Rose et al., 2001). The two kinds of LVADs, both pulsatile flow VADs (PF-VADs) and continuous flow VADs (CF-VADs), are similar in terms of providing hemodynamic support and improving the quality of life and functional capacity of patients (M. S. Slaughter et al., 2009; Thohan et al., 2005). Currently, almost all implanted VADs are continuous-flow pumps because they clinically outperform older generation pulsatile flow VADs in survival rate, pump failure events, and infectious complications (Park et al., 2012; Mark S Slaughter et al., 2009). It has been estimated that LVADs could potentially be used to treat ~ 60,000 heart failure patients a year globally to improve their survival and enhance their quality of life. However, LVADs are greatly under-utilized with ~3000 LVADs implanted in the US every year due to the risk of adverse events associated with LVAD use (Molina et al., 2021). Specifically, CF-VADs create non-physiological stimuli, due to diminished pressure and flow pulsatility, and have been associated with adverse events including increased risk of hemolysis and pump thrombosis due to supraphysiological shear induced platelet activation (Chen et al., 2018; Katharine H. Fraser, Tao Zhang, M. Ertan Taskin, Bartley P. Griffith, & Zhongjun J. Wu, 2012), and non-surgical bleeding, particularly in the gastrointestinal (GI) tract (Chen, Sun, Wang, Fan, & Deng, 2019; Cushing & Kushnir, 2016). While still major challenges, hemolysis and pump thrombosis have been mitigated through LVAD designs that reduce pump shear stress and residence times, positioning of the outflow cannula, and anticoagulant therapies (K. H. Fraser, T. Zhang, M. E. Taskin, B. P. Griffith, & Z. J. Wu, 2012). Non-surgical bleeding remains a frequent complication in patients supported with CF-VADs (18%–40% of patients) (Aggarwal et al., 2012; John et al., 2011; Morgan et al., 2012), requiring transfusion of blood products (2–4 units) (Birks, 2017), and hospitalization (average cost is $19,465) (Eckman & John, 2012).

Although non-surgical bleeding in CF-VAD patients is a multifactorial problem and there is an incomplete understanding of the underlying mechanisms, clinical data suggest that the development of Acquired von Willebrand factor syndrome (AVWS) and the formation of Arteriovenous Malformations (AVMs) are major risk factors (Crow et al., 2010; Demirozu et al., 2011; Guha, Eshelbrenner, Richards, & Monsour Jr, 2015; Patel, Vukelic, & Jorde, 2016; Uriel et al., 2010). One aspect that is likely underreported is the influence of AVWS on increased stroke risk in LVADs patients, as many physicians typically reduce the anticoagulation and antiplatelet therapies in these patients in an effort to alleviate the repeated non-surgical bleeding that occurs due to vWF dysregulation. Thus, AVWS induced adverse events lead to decreased quality of life and diminished enthusiasm for life-extending technologies like CF-VAD. Therefore, it is important to identify biomarkers

associated with loss of pulsatility like endothelial von Willebrand factor (vWF) and pro-inflammatory/pro-angiogenic soluble factors for identification of biomarkers sensitive to pulsatility. Biomarkers sensitive to pulsatility can be useful to rapidly identify and monitor patients at high risk of non-surgical bleeding following CF-VAD placement. They can also serve as biomarkers to determine optimal parameters for CF-VAD flow modulation protocols or other therapies that can mitigate non-surgical bleeding events.

Small animal models do not faithfully replicate human physiology and studies with large animal models like young calves and pigs does not result in non-surgical bleeding. These models are also not representative of the aging heart failure population that typically receives LVADs. Therefore, identification and validation of biomarkers sensitive to pulsatility requires a physiologically relevant model, capable of replicating the physiology of HF patients. In this study, we adopted a human vessel-on-a-chip model, here called the Vascular Pulse Pressure Model (VPPM), that enables culture of human endothelial cells under conditions that simulate vascular pressure and flow pulsatility of patients with and without CF-VAD support. We used the VPPM to identify biomarkers that respond to physiologic and diminished pulsatility. In this study, we validated VPPM-identified biomarkers of pulsatility against biomarkers identified in blood samples collected from CF-VAD patients, pre- and post- CF-VAD implant and refined our list to biomarkers that show similar behavior both in-vitro and in patients.

MATERIALS AND METHODS

Microfabrication and Setup of VPPM

The VPPM is a unique closed-loop model developed in our lab based on principles of existing mock flow loops designed to mimic a human circulatory system and adapted for the culture of human endothelial cells. Previously, the VPPM has been validated to recreate physiologic flow and disturbed flow for various applications in cardiovascular disease modeling and drug testing (Donoghue, Nguyen, Graham, & Sethu, 2021; Estrada, Giridharan, Nguyen, Prabhu, & Sethu, 2011; Estrada, Giridharan, Nguyen, Roussel, et al., 2011; Tran-Nguyen et al., 2020). In this study, the VPPM was adopted for the culture of human endothelial cells and identify biomarkers sensitive to pulsatility.

For each VPPM, a microfluidic device (Figure 1A) was fabricated to function as cell culture chamber. First, the architecture of this device was designed using SolidWorks, and then printed into molds via Stereolithography (SLA) 3D printing with Ceramic-Like Advanced High Temp White (PerFORM) material at Protolabs, USA. One mold was used to build the device's top piece with a microfluidic channel that is 300 μm tall and 5 mm wide. A second mold was used to produce thin bottom layer. The fabrication process involves use of Polydimethylsiloxane (PDMS) monomers and curing agent (CHT USA Inc, USA) thoroughly mixed and filled into both molds at a ratio of 10:1, degassed under vacuum for 60 mins, cured at room temperature overnight, and then heated to 70°C for 30 mins for complete polymerization of PDMS. The top PDMS piece was removed from its mold and two access holes were punched to create an inlet and an outlet. Prior to removing the thin membrane from its mold, both components were treated with oxygen plasma (Plasma Cleaner PDC-001, Harrick Plasma, USA), quickly pressed together, and heated on a hotplate

at 100°C for 5 min to ensure irreversible bonding and hermetic sealing. The final product tested for leaks or defects.

Other VPPM essential components are presented in Figure 1B, including a pressure sensor (Validyne Engineering, USA), a flow sensor (Transonic Systems Inc., USA), a custom pumping component containing flexible Penrose tubing, a Keck-tubing clamp (Duran Group, Switzerland) acting as a resistance element, various types of tubing (Masterflex, USA), multiple one-way valves and three-way valves, syringes, and connectors. Prior to use, all VPPM components were sterilized by either autoclave or Ethylene Oxide gas (Anderson Sterilizers Inc., USA).

VPPM assembly was performed in a sterile environment (1300 Series A2 safety cabinet, Thermo Scientific, USA), and transferred to a large incubator (Norlake Scientific, USA) for culture. A pulsatile pneumatic pump (LB Engineering, Germany) located outside the incubator drove fluid flow in the VPPM via the pump component. The pneumatic pump pressure and frequency, the VPPM resistance element, and the air compliance were carefully adjusted together to obtain the desired pressure and flow waveforms for either normal pulsatile flow or flow with diminished pulsatility. Pressure and flow sensors were connected to LabView for real-time monitoring. Mean cell culture chamber wall shear stress was calculated to be within ~ 10–15 dyne/cm^2 at the target flow rate and stretch was maintained within 6–10% via regular observation in both conditions. The incubator was operated at 37°C and in a 5% CO_2 environment.

Seeding of human endothelial cells into VPPM

Prior to seeding, a sterile PDMS microfluidic device was coated with 15 μL/mL human fibronectin (Corning, USA) and incubated for at least 30 mins at 37ºC to facilitate strong cell attachment. Primary adult human aortic endothelial cells (HAECs) (Cat#: PCS-100–011, ATCC, USA) were regularly cultured using Endothelial Cell Growth Medium EGM-2 Bullet Kit (Lonza, USA) at 37°C with 5% CO_2 until reaching the desired confluency and sufficient quantity.

For seeding, HAECs were dissociated using 0.05% Trypsin-EDTA (Gibco, Canada), incubation at 37°C for 4 mins, and the dissociated cells were centrifuged at 200×g for 5 mins. The viable cell number was estimated using a Countess II instrument (Invitrogen, USA). Approximately 4×10^6 cells were seeded into each PDMS microfluidic device by injecting the appropriate volume of cell suspension using sterile syringes attached to a syringe needle. After seeding, a small, sterilized metal stopper was used to seal the outlet to stop fluid flow and prevent the loss of seeded cells. The device was incubated at 37°C with a 5% CO_2 level for 1–2 days until HAECs were evenly distributed to attain a confluent monolayer. For each in-vitro VPPM study, approximately 15 mL of EGM-2 cell culture medium, supplemented with 2% Penicillin-Streptomycin (Gibco, USA), was used for perfusion. Cell phenotypes were observed at the end of the experiments and images were taken using a Nikon Eclipse TE2000-U epifluorescence microscope (Nikon Instrument Inc., USA) (Figure 1C).

Profiling of biomarkers in-vitro

For sample collection, the cell culture medium from successfully completed VPPM experiments was collected and stored at −80°C until use. For cytokine assays, vWF level was measured using Human vWF ELISA Kit (Cat #: RAB0556, Sigma-Aldrich, USA), according to protocols designed by the manufacturer. Pro-inflammatory / pro-angiogenic cytokine levels were measured using Human High Sensitivity Discovery Assay (i.e., HDHSTC14) at Eve Technologies Ltd., Canada. The HDHSTC14 panel measured Granulocyte-macrophage colony-stimulating factor (GM-CSF), Interferon-gamma (IFNy), Interleukin 1-beta (IL-1β), IL-2, IL-4, IL-5, IL-6, IL-8, IL-10, IL-12p70, IL-13, IL-17A, IL-23, and Tumor Necrosis Factor-alpha (TNF-α). The Angiopoietin-2 (ANGPT-2) level was additionally measured using Human Angiopoietin-2 ELISA Kit (Cat #: RAB0016, Sigma-Aldrich, USA). All samples were run in duplicates, and average values were used for data analysis.

Profiling of biomarkers in CF-VAD patients

Blood samples were collected from patients selected for CF-VAD placement via an ongoing UAB IRB protocol #: IRB-300003505 in coordination with the heart failure unit at UAB hospital. Patient blood was obtained around 1–2 days before CF-VAD placement and monthly following CF-VAD implant using 4 mL blood collection tubes (green-capped, Lithium Heparin coated BD Vacutainer (BD, Cat # 367884, USA). Blood samples were centrifuged at 960×g for 15 mins at room temperature to extract plasma. Patient plasma samples were stored in 2 mL Eppendorf tubes at −80°C until use. Patients' personal information was coded to protect their identity and avoid bias in data analysis.

For cytokine assays, vWF level was measured using Human vWF ELISA Kit (Cat #: RAB0556, Sigma-Aldrich, USA), according to manufacturer protocol. Pro-inflammatory / pro-angiogenic cytokine levels were measured using Human High Sensitivity Discovery Assay (HDHSTC14) and Human Angiogenesis & Growth Factor Discovery Assay (HDAGP17) at Eve Technologies Ltd., Canada. The HDAGP17 panel measured Angiopoietin-2 (ANGPT-2), Bone Morphogenetic Protein-9 (BMP-9), Epidermal Growth Factor (EGF), Endoglin, Endothelin-1, Fibroblast Growth Factor 1 (GFG-1), GFG-2, Follistatin, Granulocyte Colony-Stimulating Factor (G-CSF), Heparin-binding EGF-like growth factor (HB-EGF), Hepatocyte Growth Factor (HGF), IL-6, IL-8, Leptin, Vascular Endothelial Growth Factor A (VEGF-A), VEGF-C, and VEGF-D. All samples were run in duplicates, and average values were used for data analysis.

Data analysis and Statistical study

Data is represented as mean ± SEM. GraphPad PRISM™ 9 software was used to perform statistical analysis and prepare reported graphs. Student's unpaired t-test was used for comparison of in-vitro data and student's paired t-test was used for two-group comparison of data observed in patient samples. Two-tailed statistical significance was set at $p<0.05$. In graphs, (*) denotes for $p<0.05$ and (**) for $p<0.01$.

RESULTS

Characterization of VPPM-generated flows

With real-time pressure and flow waveforms recorded using electronic sensors integrated within the VPPM flow loop, we were able to generate hemodynamic profiles of our experimental conditions. The VPPM was able to generate pulsatile pressure and flow profiles similar to those under normal blood flow in the arterial system and those seen in arteries of advanced heart failure patients implanted with CF-VADs (Figure 2A). Specifically, VPPM-generated normal pulsatile flow seen in healthy individuals (referred as Normal Pulsatile Flow), where physiologic pulse pressure was maintained close to 40 mmHg, and systolic / diastolic pressure was maintained at 120 / 80 mmHg. VPPM-generated Normal Pulsatile Flow had peak flow rates around 40 mL/min with periods of no flow. In contrast, VPPM-generated flow with diminished pulsatility (referred to as CF-VAD Continuous Flow) was characterized by a diminished pulse pressure of ~5 mmHg and systolic/diastolic pressure maintained at 110 / 105 mmHg. The flow rate fluctuated between 8 – 18 mL/min. Both conditions were run at the same pumping frequency of 60 bpm. Numerical profiles of both flows are summarized in Figure 2B.

Identification of biomarkers in-vitro

Results from our in-vitro study using VPPM with the culture of primary adult HAECs suggested that 72-hour diminished pulsatility remarkably affects endothelial production of vWF, ANGPT-2, (Figure 3). Specifically, exposure to continuous flow resulted in 45% decrease in vWF level from a mean value of 9.80 ± 1.107 ng/mL to 5.32 ± 1.333 ng/mL (n=5, p=0.0327) and approximately 3-fold increase of ANGPT-2 from a mean value of 775.29 ± 184.9 pg/mL to 2471.93 ± 635.4 pg/mL (n=5, p=0.0334) in the perfused cell culture medium. In addition, IL-6 and IL-8 decreased slightly from 132.9 ± 18.82 pg/mL to 104.9 ± 58.97 and from 656.1 ± 70.81 pg/mL to 574.2 ±214.3 respectively, although without statistical significance (n=3).

Validation of biomarkers against evaluation of patient samples

The patient's plasma level of von Willebrand factor (vWF) were also measured using their pre-VAD (referred to as Baseline) and post-VAD plasma samples of one, two, three months (Figure 4A). Similar to in-vitro results, the evaluation of patient samples suggests that the patient's plasma vWF level decreases ~ 50%, from a mean value of 45.59 ± 8.254 μg/mL at baseline to 22.49 ± 3.85 μg/mL (n=15, p=0.0012) after one month of CF-VAD support (m1 post-VAD). Interestingly, this reduced level remained unchanged for additional two months with the mean vWF level of 26.96 ± 5.526 μg/mL after two months post-VAD and of 23.75 ± 5.754 μg/mL after three months post-VAD (p=0.068 for both cases compared to baseline level).

In addition, more than 30 different pro-inflammatory and pro-angiogenic cytokines were screened using plasma samples collected 1–2 days before CF-VAD implant for patient baseline and a month after CF-VAD implant for post-VAD soluble factor levels. The results showed that most pro-inflammatory/pro-angiogenic soluble factors had either insignificant or random changes post-VAD compared to baseline levels. These results were not surprising

because CF-VAD patients were often severely ill, on multiple medications, and had comorbidities that could influence their clinical outcomes to an additional major treatment like CF-VAD in unpredictable ways. However, it is noteworthy that there was a statistically significant increase of 64% in patient plasma level changes of ANGPT-2 level from a mean value of 7074 ± 1715 pg/mL to that of 11615 ± 1967 pg/mL (n=8, p=0.0376), (Figure 4B) in agreement with in-vitro results. Patients' plasma level of IL-6 decreased 27% with statistical significance from 9.93 ± 1.497 pg/mL to 7.224 ± 1.309 pg/mL (n=8, p=0.0186) similar to the trend of change seen in-vitro. Patients' plasma level of IL-8 increased 62% from 22.48 ± 2.464 pg/mL to 36.34 ± 9.743 pg/mL, but without statistical significance (n=8, p=0.1148) (Figure 4C). Interestingly, patient's plasma level of TNF-α also increased substantially by 52% from 9.834 ± 1.104 pg/mL to 15.01 ± 2.236 pg/mL (n=8, p=0.0220), making it another candidate biomarker for identifying CF-VAD patients at high risk of non-surgical bleeding. However, the level of TNF-a was too small within VPPM for detectable results and in-vitro validation. This might be because TNF-α is mainly produced by immune cells (e.g., macrophages, T lymphocytes and natural killer cells) and not by aortic endothelial cells.

DISCUSSION / CONCLUSION

There is growing evidence that the diminished pulsatility associated with CF-VAD support plays a critical role in the development of non-surgical bleeding. The arterial endothelium represents the primary location where the effects of diminished pulsatility manifest on the arterial endothelial cells that line the arterial vessels. Our prior work demonstrated that the diminished pulsatility leads to dysfunction of HAECs and triggers acute pro-inflammatory/pro-angiogenic responses (Haglund et al., 2019; Nguyen et al., 2022; Patibandla et al., 2016). The goal of this study was to profile endothelial vWF and pro-inflammatory/pro-angiogenic soluble factors for identification of biomarkers sensitive to pulsatility. The VPPM allows us to screen for these biomarkers in a physiologically relevant and highly controlled conditions (without other cofounding factors). The comparison of soluble factor level changes in vitro and in patient plasma samples establishes meaningful correlations that helped validate VPPM-identified biomarkers as reliable and sensitive to pulsatility.

Our study results identified ANGPT-2 and vWF as highly sensitive to pulsatility, along with IL-6, IL-8, and TNF- α as other promising biomarker candidates. Furthermore, published literature supports our clinical observations. Concerning pro-inflammatory/pro-angiogenic responses, ANGPT-2, TNF- α, and IL-8 were reported to be significantly higher in patients on CF-VAD support compared to their healthy baseline levels, patients on pulsatile flow-VAD, or patients having a heart transplant (Grosman-Rimon et al., 2015; Jeske et al., 2014; Tabit et al., 2016; Truby & Topkara, 2016). Elevated levels of ANGPT-2 and TNF-α were also associated with AVMs and bleeding events not limited to VADs (Kim et al., 2018; Patel et al., 2016; Tabit et al., 2018). In addition, direct visualization studies of vWF suggest that diminished pulsatility as seen with CF-VAD, significantly increased the unraveling and elongation of surface-bound vWF molecules (analogous to endothelial cell-bound vWF) ($p<0.05$), which can potentially enhance cleavage of vWF into low molecular weight (MW) multimers (Wang et al., 2022). There is also evidence that loss of pulsatility may reduce production of vWF (need Vincent et al. reference here) and that loss of high MW vWF due

to diminished pulsatility also caused endothelial dysfunction (Bartoli et al., 2018; Kang et al., 2017).

Prior to translation of any promising treatment strategies to mitigate loss of pulsatility related adverse events with CF-VAD support, extensive evaluation of the physiological effects of artificial pulsatility on the circulatory system needs to be accomplished using relevant models. Unfortunately, small animal models do not faithfully simulate human disease and are not large enough to accommodate CF-VADs. While large animal models (calves and pigs) are comparable in size and anatomical structure, and can be used to establish stable and irreversible HF, (Monreal et al., 2014), non-surgical bleeding events associated with diminished pulsatility in CF-VAD support are rarely seen in these models as they do not mimic the effects of aging seen in human VAD recipients. Moreover, quadrupedal large animals (calf, pigs, sheep etc.) that are used to mimic human HF models have vascular impedances that are markedly different from bipedal humans (Koenig et al., 2008). Since the arterial endothelium is the major transducer of pulsatility in the body, a vascular cell culture model constructed using human endothelial cells could possibly serve as a viable and cost-effective model to accomplish early-stage evaluation of promising treatments, which can then be evaluated for safety in animal models prior to being implemented in patients. However, to truly mimic effects of diminished pulsatility in-vitro, evaluation of arterial endothelial cells needs to be accomplished in an environment that mimics critical aspects of flow pulsatility including pulse pressure, shear stress, and stretch. Arterial endothelial cells rely on these mechanical stress signals seen during hemodynamic loading and unloading as feedback mechanisms to maintain normal homeostasis. To overcome shortcomings with available systems for culture of endothelial cells, the VPPM platform was designed to culture endothelial cells under realistic mechanical loading conditions and in vivo-like pressure and flow patterns. The VPPM cell culture channel represents a circumferential section of the aortic wall and accurately represents the physiological values for flow, pressure, stretch, and shear stress on the aortic section (Estrada, Giridharan, Nguyen, Roussel, et al., 2011). Importantly, the VPPM also allows in-vitro study of diminished pulsatility in highly controlled conditions to evaluate potential treatments like flow modulation or therapeutic drugs. Limitations with animal models can possibly be overcome via use of the VPPM platform with in-vitro culture of primary human adult endothelial cells and represents a viable alternative for testing of different treatment options to mitigate the adverse events associated with loss of pulsatility. This study is particularly significant as it clearly identifies biomarkers (ANGPT-2 and vWF) where changes within the VPPM mirror changes seen in patients prior to and post- CF-VAD placement and can potentially serve as biomarkers to evaluate pulsatility effects and to identify/optimize promising treatments prior to clinical use.

Limitations of our study include a small in-vitro sample size (3–5 replications), and duration of the in-vitro study (72-hours). This possibly prevented us the observation of statistical significance with biomarker candidates that showed consistent trends with diminished pulsatility (a type II statistical error). Despite these limitations, the VPPM provides a controlled, high throughput platform that can enable identification of biomarkers and mechanisms, and evaluation of therapies.

Source of Funding:

This study was enabled by the generous support from the National Institutes of Health (1R01HL151663) and the National Science Foundation (2004475).

ABBREVIATIONS

ANGPT-2	Angiopoietin-2
ASYN	asynchronous
AVMs	Arteriovenous Malformations
AVWS	Acquired von Willebrand factor syndrome
CF-VAD	Continuous-Flow Ventricular Assist Device
HAECs	Human Aortic Endothelial Cells
HF	Heart failure
IL-6	Interleukin 6
IL-8	Interleukin 8
LVADs	Left Ventricular Assist Devices
MW	molecular weight
PDMS	Polydimethylsiloxane
SYN	synchronous
TNF-α	Tumor Necrosis Factor alpha
VPPM	Vascular Pulse Pressure Model
vWF	von Willebrand factor

REFERENCES

Aggarwal A, Pant R, Kumar S, Sharma P, Gallagher C, Tatooles AJ, . . . Bhat G. (2012). Incidence and management of gastrointestinal bleeding with continuous flow assist devices. Ann Thorac Surg, 93(5), 1534–1540. doi:10.1016/j.athoracsur.2012.02.035 [PubMed: 22541185]

Bartoli CR, Zhang DM, Hennessy-Strahs S, Kang J, Restle DJ, Bermudez C, . . . Acker MA. (2018). Clinical and in vitro evidence that left ventricular assist device–induced von Willebrand factor degradation alters angiogenesis. Circulation: Heart Failure, 11(9), e004638. [PubMed: 30354363]

Birks EJ (2017). Stopping LVAD Bleeding. Circulation Research, 121(8), 902–904. doi:doi:10.1161/CIRCRESAHA.117.311759 [PubMed: 28963184]

Chen Z, Jena SK, Giridharan GA, Koenig SC, Slaughter MS, Griffith BP, & Wu ZJ (2018). Flow features and device-induced blood trauma in CF-VADs under a pulsatile blood flow condition: A CFD comparative study. International journal for numerical methods in biomedical engineering, 34(2), 10.1002/cnm.2924. doi:10.1002/cnm.2924

Chen Z, Sun A, Wang H, Fan Y, & Deng X (2019). Non-physiological shear stress-induced blood damage in ventricular assist device. Medicine in Novel Technology and Devices, 3, 100024. doi:10.1016/j.medntd.2019.100024

Crow S, Chen D, Milano C, Thomas W, Joyce L, Piacentino III,V., . . . Bowles D. (2010). Acquired von Willebrand syndrome in continuous-flow ventricular assist device recipients. The Annals of thoracic surgery, 90(4), 1263–1269. [PubMed: 20868825]

Cushing K, & Kushnir V (2016). Gastrointestinal Bleeding Following LVAD Placement from Top to Bottom. Digestive diseases and sciences, 61(6), 1440–1447. doi:10.1007/s10620-016-4123-4 [PubMed: 27017225]

Demirozu ZT, Radovancevic R, Hochman LF, Gregoric ID, Letsou GV, Kar B, . . . Frazier O. (2011). Arteriovenous malformation and gastrointestinal bleeding in patients with the HeartMate II left ventricular assist device. The Journal of heart and lung transplantation, 30(8), 849–853. [PubMed: 21530318]

Donoghue L, Nguyen KT, Graham C, & Sethu P (2021). Tissue chips and microphysiological systems for disease modeling and drug testing. Micromachines, 12(2), 139. [PubMed: 33525451]

Eckman PM, & John R (2012). Bleeding and thrombosis in patients with continuous-flow ventricular assist devices. Circulation, 125(24), 3038–3047. doi:10.1161/circulationaha.111.040246 [PubMed: 22711669]

Estrada R, Giridharan GA, Nguyen M-D, Prabhu SD, & Sethu P (2011). Microfluidic endothelial cell culture model to replicate disturbed flow conditions seen in atherosclerosis susceptible regions. Biomicrofluidics, 5(3), 032006.

Estrada R, Giridharan GA, Nguyen M-D, Roussel TJ, Shakeri M, Parichehreh V, . . . Sethu P. (2011). Endothelial cell culture model for replication of physiological profiles of pressure, flow, stretch, and shear stress in vitro. Analytical chemistry, 83(8), 3170–3177. [PubMed: 21413699]

Fraser KH, Zhang T, Taskin ME, Griffith BP, & Wu ZJ (2012). A quantitative comparison of mechanical blood damage parameters in rotary ventricular assist devices: shear stress, exposure time and hemolysis index. Journal of biomechanical engineering, 134(8), 081002–081002. doi:10.1115/1.4007092 [PubMed: 22938355]

Fraser KH, Zhang T, Taskin ME, Griffith BP, & Wu ZJ (2012). A quantitative comparison of mechanical blood damage parameters in rotary ventricular assist devices: shear stress, exposure time and hemolysis index. Journal of biomechanical engineering, 134(8), 081002. doi:10.1115/1.4007092 [PubMed: 22938355]

Grosman-Rimon L, Jacobs I, Tumiati LC, McDonald MA, Bar-Ziv SP, Fuks A, . . . Shogilev DJ. (2015). Longitudinal assessment of inflammation in recipients of continuous-flow left ventricular assist devices. Canadian Journal of Cardiology, 31(3), 348–356. [PubMed: 25746024]

Guha A, Eshelbrenner CL, Richards DM, & Monsour HP Jr (2015). Gastrointestinal bleeding after continuous-flow left ventricular device implantation: review of pathophysiology and management. Methodist DeBakey cardiovascular journal, 11(1), 24. [PubMed: 25793026]

Haglund TA, Rajasekaran NS, Smood B, Giridharan GA, Hoopes CW, Holman WL, . . . Tallaj JA. (2019). Evaluation of flow-modulation approaches in ventricular assist devices using an in-vitro endothelial cell culture model. The Journal of Heart and Lung Transplantation, 38(4), 456–465. [PubMed: 30503074]

Jeske W, Syed D, Escalante V, Coglianese E, Schwartz J, & Walenga JM (2014). Inflammatory cytokines are upregulated in patients with implanted ventricular assist devices. In: American Society of Hematology Washington, DC.

John R, Kamdar F, Eckman P, Colvin-Adams M, Boyle A, Shumway S, . . . Liao K. (2011). Lessons learned from experience with over 100 consecutive HeartMate II left ventricular assist devices. Ann Thorac Surg, 92(5), 1593–1599; discussion 1599–1600. doi:10.1016/j.athoracsur.2011.06.081 [PubMed: 22051256]

Kang J, Hennessy-Strahs S, Kwiatkowski P, Bermudez CA, Acker MA, Atluri P, . . . Bartoli CR. (2017). Continuous-flow LVAD support causes a distinct form of intestinal angiodysplasia. Circulation research, 121(8), 963–969. [PubMed: 28729354]

Kim G, Sayer G, Ransom J, Keebler M, Katz J, Kilic A, . . . Brieke A. (2018). Increased Bleeding Risk in LVAD Patients with Elevated Angiopoetin-2 and TNF-α: Analysis of the PREVENT Multicenter Study. The Journal of Heart and Lung Transplantation, 37(4), S71.

Koenig SC, Giridharan GA, Ewart DL, Schroeder MJ, Ionan C, Slaughter MS, . . . Prabhu SD. (2008). Human, bovine and porcine systematic vascular input impedances are not equivalent:

implications for device testing and xenotransplantation in heart failure. The Journal of heart and lung transplantation, 27(12), 1340–1347. [PubMed: 19059115]

McLarty A (2015). Mechanical circulatory support and the role of LVADs in heart failure therapy. Clinical Medicine Insights: Cardiology, 9, CMC. S19694.

Molina EJ, Shah P, Kiernan MS, Cornwell III WK, Copeland H, Takeda K, . . . Jacobs JP. (2021). The society of thoracic surgeons intermacs 2020 annual report. The Annals of thoracic surgery, 111(3), 778–792. [PubMed: 33465365]

Monreal G, Sherwood LC, Sobieski MA, Giridharan GA, Slaughter MS, & Koenig SC (2014). Large animal models for left ventricular assist device research and development. ASAIO Journal, 60(1), 2–8. [PubMed: 24270232]

Morgan JA, Paone G, Nemeh HW, Henry SE, Patel R, Vavra J, . . . Brewer RJ. (2012). Gastrointestinal bleeding with the HeartMate II left ventricular assist device. J Heart Lung Transplant, 31(7), 715–718. doi:10.1016/j.healun.2012.02.015 [PubMed: 22425231]

Nguyen KT, Donoghue L, Giridharan GA, Naber JP, Vincent D, Fukamachi K, . . . Sethu P. (2022). Acute response of human aortic endothelial cells to loss of pulsatility as seen during cardiopulmonary bypass. Cells Tissues Organs, 211(3), 1–11. [PubMed: 34438405]

Park SJ, Milano CA, Tatooles AJ, Rogers JG, Adamson RM, Steidley DE, . . . Slaughter MS. (2012). Outcomes in advanced heart failure patients with left ventricular assist devices for destination therapy. Circulation: Heart Failure, 5(2), 241–248. [PubMed: 22282104]

Patel SR, Vukelic S, & Jorde UP (2016). Bleeding in continuous flow left ventricular assist device recipients: an acquired vasculopathy? Journal of Thoracic Disease, 8(10), E1321. [PubMed: 27867617]

Patibandla PK, Rajasekaran NS, Shelar SB, Giridharan GA, Litovsky SH, & Sethu P (2016). Evaluation of the effect of diminished pulsatility as seen in continuous flow ventricular assist devices on arterial endothelial cell phenotype and function. The Journal of Heart and Lung Transplantation, 35(7), 930–932. [PubMed: 27138701]

Rose EA, Gelijns AC, Moskowitz AJ, Heitjan DF, Stevenson LW, Dembitsky W, . . . Levitan RG. (2001). Long-term use of a left ventricular assist device for end-stage heart failure. New England Journal of Medicine, 345(20), 1435–1443. [PubMed: 11794191]

Slaughter MS, Rogers JG, Milano CA, Russell SD, Conte JV, Feldman D, . . . Long JW. (2009). Advanced heart failure treated with continuous-flow left ventricular assist device. New England Journal of Medicine, 361(23), 2241–2251. [PubMed: 19920051]

Slaughter MS, Rogers JG, Milano CA, Russell SD, Conte JV, Feldman D, . . . Frazier OH. (2009). Advanced heart failure treated with continuous-flow left ventricular assist device. N Engl J Med, 361(23), 2241–2251. doi:10.1056/NEJMoa0909938 [PubMed: 19920051]

Tabit CE, Chen P, Kim GH, Fedson SE, Sayer G, Coplan MJ, . . . Liao JK. (2016). Elevated angiopoietin-2 level in patients with continuous-flow left ventricular assist devices leads to altered angiogenesis and is associated with higher nonsurgical bleeding. Circulation, 134(2), 141–152. [PubMed: 27354285]

Tabit CE, Coplan MJ, Chen P, Jeevanandam V, Uriel N, & Liao JK (2018). Tumor necrosis factor-α levels and non-surgical bleeding in continuous-flow left ventricular assist devices. The Journal of Heart and Lung Transplantation, 37(1), 107–115. [PubMed: 28651907]

Thohan V, Stetson SJ, Nagueh SF, Rivas-Gotz C, Koerner MM, Lafuente JA, . . . Torre-Amione G. (2005). Cellular and hemodynamics responses of failing myocardium to continuous flow mechanical circulatory support using the DeBakey-Noon left ventricular assist device: a comparative analysis with pulsatile-type devices. J Heart Lung Transplant, 24(5), 566–575. doi:10.1016/j.healun.2004.02.017 [PubMed: 15896754]

Tran-Nguyen TK, Chandra D, Yuan K, Patibandla PK, Nguyen KT, Sethu P, . . . Kim Y.-i. (2020). Glucose-regulated protein 78 autoantibodies are associated with carotid atherosclerosis in chronic obstructive pulmonary disease patients. Immunohorizons, 4(2), 108–118. [PubMed: 32086320]

Truby LK, & Topkara VK (2016). Angiopoietin-2: marker or mediator of angiogenesis in continuous-flow left ventricular assist device patients? Journal of thoracic disease, 8(11), 3042. [PubMed: 28066578]

Uriel N, Pak S-W, Jorde UP, Jude B, Susen S, Vincentelli A, . . . Mancini D. (2010). Acquired von Willebrand syndrome after continuous-flow mechanical device support contributes to a high prevalence of bleeding during long-term support and at the time of transplantation. Journal of the American College of Cardiology, 56(15), 1207–1213. [PubMed: 20598466]

Wang Y, Nguyen KT, Ismail E, Donoghue L, Giridharan GA, Sethu P, & Cheng X (2022). Effect of pulsatility on shear-induced extensional behavior of Von Willebrand factor. Artificial Organs, 46(5), 887–898. [PubMed: 34866200]

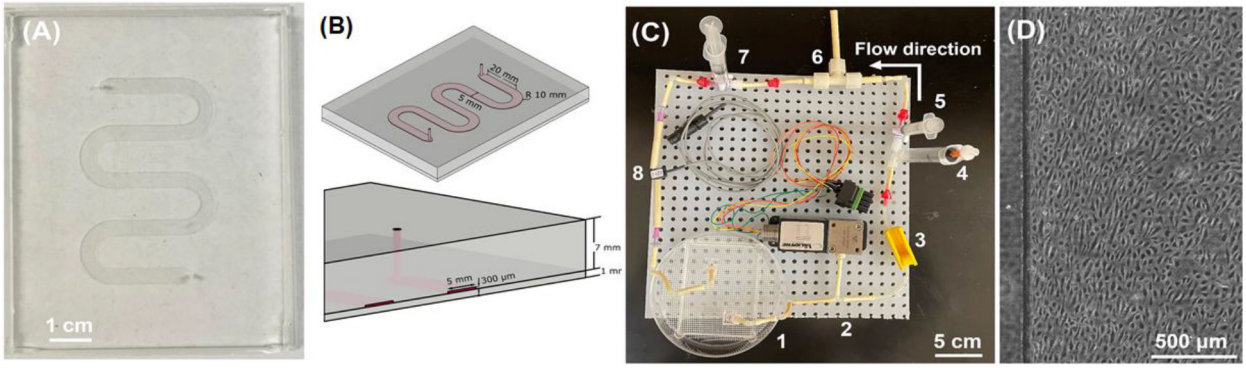

Figure 1:

A—PDMS microfluidic device fabricated to function as VPPM cell culture chamber. **B—**VPPM Setup with its essential components that include: (1) syringe to inject cell culture medium into the closed-loop, (2) built-in pump connector, (3) syringe to provide air compliance, (4) flow sensor, (5) VPPM microfluidic cell culture chamber, (6) pressure sensor, (7) Keck-tubing clamp to provide fluidic resistance that increases baseline pressure, (8) syringe to hold perfused cell culture medium with attached air filter. Cell culture media was perfused in a counterclockwise flow direction. **C—**Microscopy imaging (4X) of seeded human endothelial cells aligned to flow direction within VPPM after 72 hours of culture under pulsatile flow. Although not reported, similar cell phenotypic response was observed with cultured human endothelial cells under flow with diminished pulsatility after 72 hours.

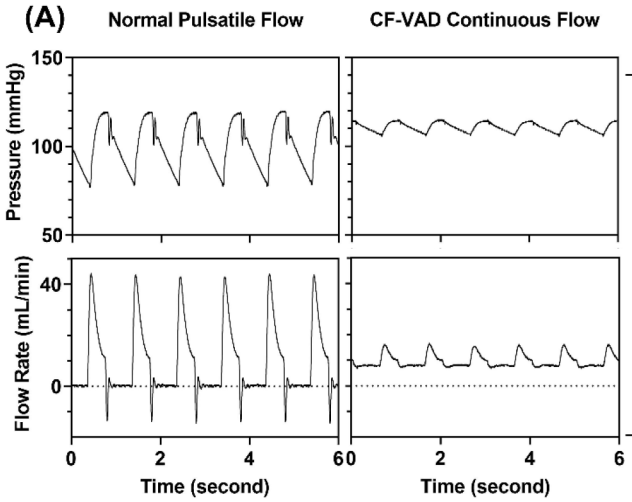

(B)

	Normal Pulsatile Flow	CF-VAD Continuous Flow
Peak Systolic Pressure (mmHg)	120	110
Diastolic Pressure (mmHg)	80	105
Pulse Pressure (mmHg)	40	5
Peak Systolic Flow Rate (mL/min)	42	18
Diastolic Flow Rate (mL/min)	0	8
Mean Flow Rate (mL/min)	10	10
Mean Wall Shear Stress (dyn/cm^2)	12	12
Pumping Frequency (bpm)	60	60

Figure 2:

(A) Panels of Pressure (mmHg) and Flow Rate (mL/min) Waveforms corresponding to VPPM-generated Normal Pulsatile Flow and Flow with diminished pulsatility as seen with CF-VAD support (CF-VAD Continuous Flow). **(B)** Numerical characteristics of VPPM-generated Normal Pulsatile Flow and CF-VAD Continuous Flow.

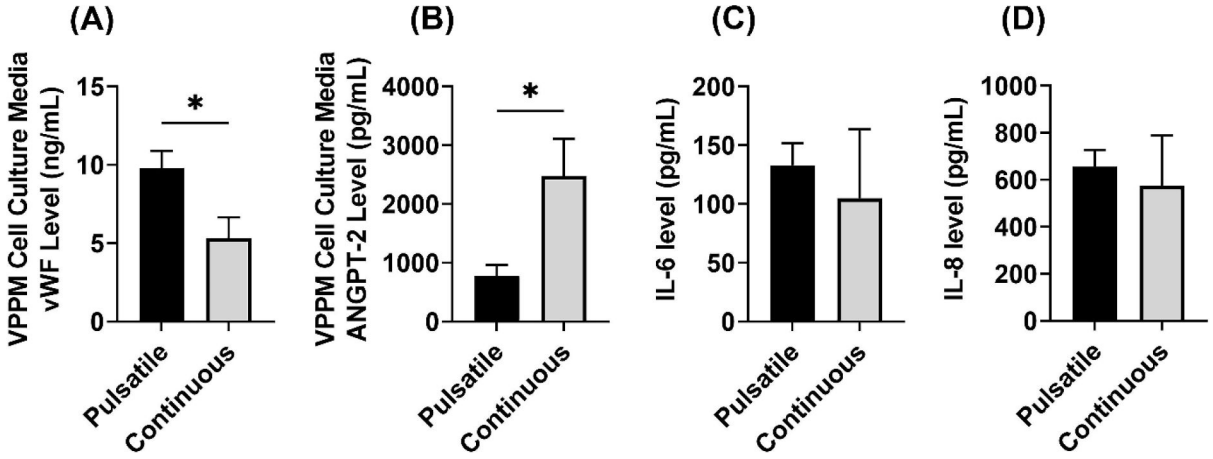

Figure 3:

Changes in VPPM perfused cell culture medium levels of pro-angiogenic/pro-inflammatory soluble factors **(A)** Angiopoietin-2 (n=5, $p<0.05$), **(B)** Interleukin-6 (n=3), **(C)** Interleukin-8 (n=3), and **(D)** von Willebrand factor (n=5, $p<0.05$). Culture medium samples were collected at the end of experiments with patient-derived HAECs cultured for 72 hours under either normal pulsatile flow (Pulsatile) or flow with diminished pulsatility as seen with CF-VAD support (Continuous).

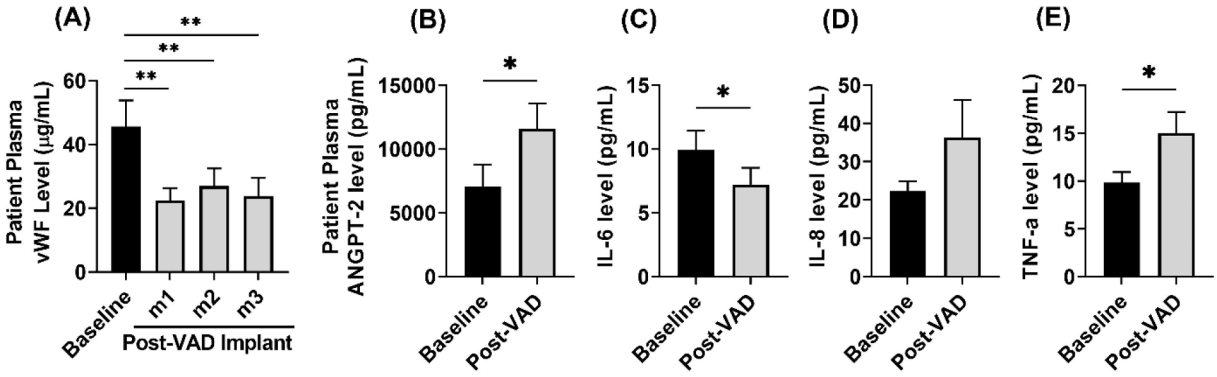

Figure 4:

Changes in CF-VAD patient plasma levels of pro-angiogenic/pro-inflammatory soluble factors (n=8), i.e., **(A)** Angiopoietin-2 ($p<0.05$), **(B)** Tumor Necrosis Factor-alpha ($p<0.05$), **(C)** Interleukin-6 ($p<0.05$), **(D)** Interleukin-8 (no statistical significance), and that of **(E)** von Willebrand factor (n=15). Patient samples were collected 1–2 days prior to CF-VAD implant (baseline), one month after implant (post-VAD) to measure levels of pro-angiogenic/pro-inflammatory soluble factors, and 1, 2, 3 months (m1, m2, m3 respectively) post-VAD implant to measure von Willebrand factor level ($p<0.01$).